Asian Journal of Electrical Sciences
ISSN: 2249-6297 (P) Vol.6 No.2, 2017, pp.1-18

DOI: https://doi.org/10.51983/ajes-2017.6.2.2001

Statistical Quality Analysis of Wavelet Based SAR Images in Despeckling Process

Prabhishek Singh[1] and Raj Shree[2]
[1]Research Scholar, [2]Assistant Professor
Department of Information Technology, Babasaheb Bhimrao Ambedkar University, Lucknow, India
E-Mail: prabhisheksingh88@gmail.com
(Received 20 May 2017; Revised 18 June 2017; Accepted 20 July 2017; Available online 27 July 2017)

Abstract **- Synthetic aperture radar (SAR) images are mainly denoised by multiplicative speckle noise, which is due to the consistent behavior of scattering phenomenon known as speckle noise. This paper presents the basic concept, role and importance of Discrete Wavelet Transform (DWT) in the field of despeckling SAR images and also offers a study of SAR image quality on applying DWT on the speckled image and log transformed speckled image. Log transform operation plays a decisive and comfortable role in despeckling SAR images as this operation changes the multiplicative behavior of the speckle noise to an additive which enables to use the additive noise restoration model efficiently. Wavelet transform has now become important in the field of image restoration although being in practice for a decade. Wavelet transform allows both time and frequency analysis simultaneously around a particular time. This transform is most appropriate for the non-stationary signals, so it deals with satellite imagery in a more efficient manner. The major part of this paper is revolving around DWT image decomposition with its role and practical implementation on the speckled image and log transformed speckled image. All the experimental results are performed on the SAR images.**
Keywords: **SAR Image, Speckle Noise, DWT, Log transformation.**

I. INTRODUCTION

Image restoration is a field of image processing which deals with recovering an original image from a degraded image. Image restoration can be defined as the process of removal of degradation in an image through linear or non-linear filtering.

Synthetic Aperture Radar is the kind of Radar that is attached to the satellites and aircraft that captures the high-resolution images of the wide surface areas of the earth. While taking these images, it deals with varying weather conditions, day and night, so a superior handling is required for these images as this situation creates a smooth noise intrusion. The kind of noise that mainly occurred in such scenario is named as the Speckle noise. SAR images are not same as optical images. Since SAR images possess the ground landscapes which is dissimilar from optical radiation, so exceptional handling is mandatory while understanding and processing the SAR images. While taking the broad regions of the landscape, SAR has to tackle with the changing weather condition, day and night. Dissimilar to optical images, SAR images are formed by the consistent interaction of the emitted microwave radiation with target areas. This consistent interaction originates arbitrary constructive and destructive nosiness resulting in salt and pepper noise all over the image.

Hence later it suffers from the effects of speckle noise. It is a granular noise that inherently exists in and degrades the quality of the active SAR image. It is a multiplicative noise, and its multiplicative nature increases the time complexity due to which computational time in image despeckling time gets increased hence the transformation of nature from multiplicative to additive is needed.

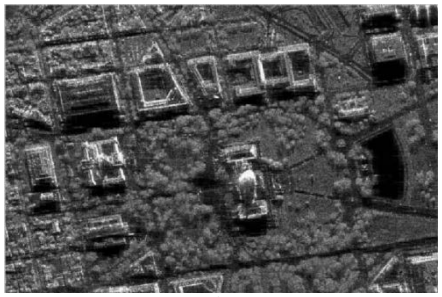

Fig.1 US Capitol beside Library of Congress, Washington, D.C.(SAR image was taken from Sandia National Laboratories.) [1]

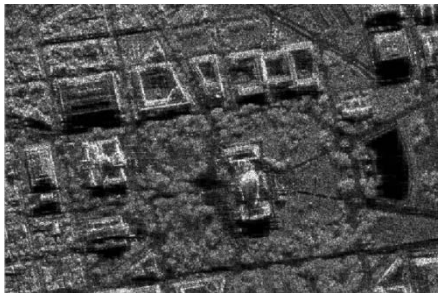

Fig.2 Noisy Image (Speckle Noise=0.2)

Real world data or signals frequently exhibits slow changing trends or oscillations punctuated with transients. On the other hand, images have smooth regions interrupted by edges or abrupt changes in contrast [2]. These sudden changes are the most important part of the data [2]. Fourier transform is a powerful tool for the data analysis. However, it does not represent sudden changes efficiently because Fourier transform represents data as a summation of sinusoidal waves which are not limited in the time and

space. These sine waves oscillate forever [2]. Therefore to accurately analyze the signals and image that have abrupt changes, we need a new class of function that is well localized in time and frequency. This brings to the concept of wavelet [2]. Many despeckling methods have been developed that remove the speckle granular pattern noise and also preserve and enhance the edge details and other features. In the domain of radar imagery, adaptive filtering techniques are efficient denoising methods including Kuan filter [3] Mean filter [4] Lee filter [5] Median filter [6] and Frost filter [7]. The issue with these conventional filtering practices is that they miss a lot of essential features although smoothens the edges and decreases the speckle noise.

There are many other methods projected which are grounded on the wavelet to diminish the speckle noise. Wavelet delivers the best way to distinct the noisy portion from the original image as the noise mainly stays in the small coefficients and vital information is present in the large coefficients and later when the wavelet thresholding is implemented then it eradicates all the small coefficient portion. Hence despeckling is achieved in a much-improved manner.

Section II discusses the previous research articles, Section III explains the basics of speckle noise and speckle noise model, Section IV describes the basics of the DWT and its importance over continuous wavelet transform, Section V presents the basic and advanced model to despeckle the SAR images using wavelet transform, Section VI shows experimental results with analysis and Conclusion is given in Section VII.

II. LITERATURE REVIEW

A mass of despeckling filters, methods and techniques can be acquired by linking the dissimilar domains of estimation (spatial, homomorphic, wavelet, and homomorphic-wavelet), the performance estimation criteria, e.g., Signal to noise ratio (SNR), minimum mean square error (MMSE) estimator, linear minimum mean square error (LMMSE), Peak signal-to-noise ratio (PSNR), minimum mean absolute error (MMAE), MAP or non-Bayesian, and the pdf models. A non- comprehensive evaluation and classification of approaches is tried in the following of this section.

Lee JS [5] in 1980 used the neighborhood pixel values in the kernel. Here each and every pixel is processed independently. Within the moving kernel, the local statistics of the pixels are taken into account. Here the weight function is evaluated by Minimum Mean Square Error estimator (MMSE). This filter efficiently removes the speckle noise but slightly degrades the details in the image.

The Frost filter [7] in 1982 is an adaptive and exponentially weighted averaging filter. An optimal minimum MSE filter is used for smoothing images. This filter is designed to smooth speckle noise and retain the important details in the image. The only drawback is it blurs the detailed information in the image.

The method by Kuan [8] in 1985 is advancement to Lee's algorithm. It is an adaptive noise smoothing filter. It is adapted to local changes in image statistics based on a Non-stationary Mean, Non-stationary Variance image model. This filter can deal with various noises which depend on signal characteristics. Also, prior knowledge about the original image is also not required. The demerit of Kuan filter is over smoothing of edges and textures.

Gagnon [9] in 1997 proposed a wavelet based de-speckling approach based on Symmetric Daubechies. It modifies the noisy wavelet coefficients according to the shrinkage rule and restores the filtered image from it. The scientist used the Elliptical soft-thresholding method. After applying the log transform and then N level transform on the image it evaluates its covariance and mean. Then inverse wavelet transform and log transformation are performed. The method reduces the speckle noise efficiently, but the computational load is increased.

A wavelet de-speckling process based on Bayesian shrinkage count on the edge details is presented in [10] in 2004.The noise-free wavelet coefficients are projected from a Bayesian wavelet shrinkage factor. Edge details are obtained using an improved ratio edge detector. These obtained statistics are later utilized in the despeckling procedure to retain edges.

Achim [11] in 2006 suggested an adaptive MAP estimator with a heavy-tailed Rayleigh signal model. The multiplicative speckle is converted into additive by applying a logarithmic transformation. Here the real and imaginary part is presumed to be described by the alpha-stable family of distribution. Another kind of statistics theory, which depends on the Mellin transform, is used to guess the model parameters from noisy observations.

Bianchi [12] in 2008 projected a procedure which depends on the GG distribution. The procedure is grounded on undecimated wavelet decomposition and MAP estimate. This paper presented an approach for dividing the wavelet coefficients based on their texture energy. This despeckling method is an enhancement to the locally adaptive GG modeling. The major disadvantage is that it undergoes from computational cost due to undecimated wavelet transform.

Wu [13] in 2010 suggested an algorithm that practices a combination of wavelet and curvelet soft thresholding method and then takes the variance between the obtained two images. This technique is capable of suppressing the speckle noise powerfully and conserves fine edges. The major flaw is that it produces blurring consequence on the image.

Christy [14] in 2013 suggested an enhancement to the prevailing Non-Local Means Filtering (NLMF) Method. A

discontinuity adaptive Non-Local Means Filtering (DA-NLMF), which practices a discontinuity adaptive weighting function, is used to preserve the edge details and delicate structures more meritoriously than the fundamental Non-Local Means. This DA-NLMF is used as efficient post-processing method along with Importance Sampling Unscented Kalman Filter (ISUKF) for despeckling SAR image. The planned method for de-speckling SAR imagery by combining ISUKF and DANLMF gives improved result than each once used separately.

Abdourrahmane Mahamane Atto, Emmanuel Trouvé, Jean-Marie Nicolas, and Thu Trang Lê [15] in 2016 presented a paper that provides statistical characteristics of wavelet operators when the thought model can be realized as the product of a deterministic piecewise regular function (signal) and a stationary random field (noise). This multiplicative observation model is analyzed in two standard frameworks, (1) direct wavelet transform of the model (2) log transform of the model prior to wavelet decomposition.

Diego Gragnaniello, Giovanni Poggi, Giuseppe Scarpa, Luisa Verdoliva, [16] in 2016 proposed a new approach to synthetic aperture radar (SAR) despeckling, based on the arrangement of multiple alternative estimates of the same data. They have given a dependable pixel-wise characterization of the image; one can take gain of this diversity by selecting the most suitable combination of estimators for each image region. Following this example, they improved a simple algorithm where only two state-of-the-art despeckling tools, characterized by complementary properties, are linearly joined.

TABLE I MAJOR CONTRIBUTION IN DESPECKLING SAR IMAGES [17]

Method	Major Contribution
Lee Filter; Refer to [18], [19], [20]	The local statistics filter, introdueced by Jong-Sen Lee in 1980, is supposedly the first despeckling filter model. The actual paper [18] contained answers for both additive signal-independent noise and speckle noise. The following solution was technologically advanced in [19] and revised in [20] together with the sigma filter.
Lee Refined Filter; Refer to [21]	This filter [21] was developed to overcome the weakness of edge boundaries which remained noisy by Lee filter. To improve filtering, once an edge is detected in a 7*7 sliding window, the algorithm uses the local gradient to estimate its orientation.
Kuan Filters; Refer to [8]	Kuan's filter [8] accurately implements the LMMSE solution [22] beginning with a signal model that features non-stationary mean and variance and thus a diagonal covariance matrix in [22]. The resulting LMMSE solution is mentioned to as local LMMSE (LLMMSE) to direct that it covers only local first order statistics, mean and variance, that is effortlessly evaluated in a sliding window.
Frost Filter; Refer to [7]	In Frost filter [7], beginning from a coherent imaging model, a parametric rough calculation of the autocorrelation function of reflectivity is resulting from local statistics. Such a function is used to devise an LMMSE solution [22] for the noise-free reflectivity itself.
MAP Filters; Refer to [23]-[27]	C-MAP filter is the model of MAP filters in the spatial domain, developed in [23] and deeply analyzed in [24]. It assumes that both the radar reflectivity and the speckle noise follow a Gamma distribution and solves the MAP equation accordingly. A refined version of the C-MAP filter that features an improved geometrical adaptivity, analogously to Lee refined filter, was proposed in [25]. This achievement marks the beginning of a certain performance saturation in spatial despeckling methods, although highly sophisticated Bayesian methods in the space domain, featuring MAP estimation associated to, e.g., Gauss-Markov and Gibbs random fields for prior modeling have been introduced later [26] and are still used [27].
Despeckling Filters and SAR Heterogeneity; Refer to [23], [28]	Tested on a simulated SAR image and an SAR-580 image [28]. The performance was way better as they efficiently average the uniform areas and preserve text, edges, linear features, and point target [23], [28].
Meer's Filter; Refer to [29]	This filter [29] considers a local neighborhood organized by a set of three concentric sliding windows, 3*3, 5*5 and 7*7. Its performances on point targets and linear features are better than Lee's refined filter which, however, is superior on linear edges.
RLP Filter; Refer to [30]-[33]	The Rational Laplacian Pyramid (RLP) filter [30] is a development for speckle filtering of the denoising method based on the enhanced Laplacian pyramid [31]. The latter is commonly used in still images for near lossless compression by exploiting quantization noise feedback [32], [33].

Homomorphic Filtering in Wavelet Domain; Refer to [34], [35]-[39]	In the wavelet-homomorphic domain, filtering has been broadly used during the last two decades and performs superior performances over conventional spatial filters [35], [36]. In fact, each wavelet subband is linked to a speckle contribution that may be exactly measured [37] and filtered out. Thus, spatially adaptive filtering becomes also scale-adaptive. Classical hard- and soft-thresholding methods [34] were applied in [38]. Thresholding based on nonlinear functions (sigmoid functions), adapted for each subband, has been used in [39].
Non-Homomorphic Filtering in Wavelet Domain; Refer to [12], [40]-[52]	Non-homomorphic filtering makes the despeckling operation faster and the algorithm easier. Non-homomorphic filtering involves applying a filtering operation to image corrupted by speckle noise without initial logarithmic transformation. Major work is done in this domain. Some improved work in this domain is discussed in detail in the articles referenced in the left-hand side.
Order Statistics and Morphological Filters; Refer to [53]-[55]	Starting with a median filter, A conditional version of median filter [53], replaces the central pixel value of the local sliding window with the sample median if and only if the former is recognized as an outlier. An adaptive version of the weighted median filter was specifically proposed for despeckling [54]. Geometric filter (GF) [55] is a powerful tool for edge-preserving smoothing of noise and especially of speckle, the purpose it was designed for.
Anisotropic Diffusion; Refer to [56]-[58]	Anisotropic diffusion [56] is a technique that aims at minimizing noise without eliminating major parts of the image, typically edges and lines or other details that are significant for the image interpretation. The derivation speckle reducing anisotropic diffusion (SRAD) is tailored to coherent images [57]. A notable application of SRAD is for coastline detection in SAR images [58].
Sigma Filter; Refer to [59], [18], [20], [60], [61]	A conceptually simple noise smoothing algorithm is the sigma filter originally developed for additive signal-independent noise [59] and promptly extended to speckle removal [18] also in comparison with local statistics filtering [20]. An enhanced version of Lee's sigma filter [60] is derived and proposed for unbiased filtering of images affected by multiplicative noise with speckle statistics. Eventually, in [61] the bias problem is solved by redefining the sigma range based on the speckle pdf.
Simulated Annealing Despeckling; Refer to [62]-[64]	Simulated Annealing (SA) was originally used for SAR image despeckling and segmentation by White [62]. SA is a stochastic optimization method. Despite its potentiality, the unlikely cartoonlike smoothness produced by SA was noticed in [63]. After that, SA was used only in conjunction with complex multivariate pdf models, like in polarimetric SAR [64].
Bilateral Filtering; Refer to [53], [65]-[67]	The bilateral filter (BF), originally introduced in [65] for grayscale images, has been recently extended to despeckling in [66]. The adaptive method in [67] exploits an order statistic filter, like [53], to reject outliers that often occur. A way to overcome such a drawback is adopting a nonlocal filtering approach.
Nonlocal Filtering; Refer to [68]-[76]	NL filtering is a generalization of the concept of data-driven weighted averaging, in which each pixel is weighted according to its similarity with the reference pixel, as in the pioneering sigma filter [68], [69]. The NL mean filter is extended in the above method [70]-[76].
Total Variation Regularization; Refer to [77]-[84]	Here, denoising is achieved through the minimization of a suitable cost function, combining a data fidelity term with a prior that enforces smoothness while preserving edges [77]. Several solutions exist to apply TV methods in the case of multiplicative noise [78]-[84].
Despeckling Based on Compressed Sensing; Refer to [86]-[88]	Sparse models are at the base of compressed sensing [85], which is the depiction of signals with some samples at a sub-Nyquist rate. Recently, some despeckling methods grounded on the compressed sensing model and sparse illustrations have appeared in [86]–[88].
Method	Major Contribution
Bayesian Methods in Spatial Domain	
Lee Filter; Refer to [18], [19], [20]	The local statistics filter, familiarized in 1980 by Jong-Sen Lee, is allegedly the first despeckling filter model. The actual paper [18] contained

	answers for both additive signal-independent noise and speckle noise. The following solution was technologically advanced in [19] and revised in [20] together with the sigma filter.
Lee Refined Filter; Refer to [21]	This filter [21] was developed to overcome the weakness of edge boundaries which remained noisy by Lee filter. To improve filtering, once an edge is detected in a 7*7 sliding window, the algorithm uses the local gradient to estimate its orientation.
Kuan Filters; Refer to [8]	Kuan's filter [8] accurately implements the LMMSE solution [22] beginning with a signal model that features non-stationary mean and variance and thus a diagonal covariance matrix in [22]. The resulting LMMSE solution is mentioned to as local LMMSE (LLMMSE) to direct that it covers only local first order statistics, mean and variance, that is effortlessly evaluated in a sliding window.
Frost Filter; Refer to [7]	In Frost filter [7], beginning from a coherent imaging model, a parametric rough calculation of the autocorrelation function of reflectivity is resulting from local statistics. Such a function is used to devise an LMMSE solution [22] for the noise-free reflectivity itself.
MAP Filters; Refer to [23]-[27]	C-MAP filter is the model of MAP filters in the spatial domain, developed in [23] and deeply analyzed in [24]. It assumes that both the radar reflectivity and the speckle noise follow a Gamma distribution and solves the MAP equation accordingly. A refined version of the C-MAP filter that features an improved geometrical adaptivity, analogously to Lee refined filter, was proposed in [25]. This achievement marks the beginning of a certain performance saturation in spatial despeckling methods, although highly sophisticated Bayesian methods in the space domain, featuring MAP estimation associated to, e.g., Gauss-Markov and Gibbs random fields for prior modeling have been introduced later [26] and are still used [27].
Despeckling Filters and SAR Heterogeneity; Refer to [23], [28]	Tested on a simulated SAR image and an SAR-580 image [28]. The performance was way better as they efficiently average the uniform areas and preserve text, edges, linear features, and point target [23], [28].

Bayesian Methods in Transform Domain	
Meer's Filter; Refer to [29]	This filter [29] considers a local neighborhood organized by a set of three concentric sliding windows, 3*3, 5*5 and 7*7. Its performances on point targets and linear features are better than Lee's refined filter which, however, is superior on linear edges.
RLP Filter; Refer to [30]-[33]	The Rational Laplacian Pyramid (RLP) filter [30] is a development for speckle filtering of the denoising method based on the enhanced Laplacian pyramid [31]. The latter is commonly used in still images for near lossless compression by exploiting quantization noise feedback [32],
Homomorphic Filtering in Wavelet Domain; Refer to [34], [35]-[39]	In the wavelet-homomorphic domain, filtering has been broadly used during the last two decades and performs superior performances over conventional spatial filters [35], [36]. In fact, each wavelet subband is linked to a speckle contribution that may be exactly measured [37] and filtered out. Thus, spatially adaptive filtering becomes also scale-adaptive. Classical hard- and soft-thresholding methods [34] were applied in [38]. Thresholding based on nonlinear functions (sigmoid functions), adapted for each subband, has been used in [39].
Non-Homomorphic Filtering in Wavelet Domain; Refer to [12], [40]-[52]	Non-homomorphic filtering makes the despeckling operation faster and the algorithm easier. Non-homomorphic filtering involves applying a filtering operation to image corrupted by speckle noise without initial logarithmic transformation. Major work is done in this domain. Some improved work in this domain is discussed in detail in the articles referenced in the left-hand side.
Non-Bayesian Approaches	
Order Statistics and Morphological Filters; Refer to [53]-[55]	Starting with a median filter, A conditional version of median filter [53], replaces the central pixel value of the local sliding window with the sample median if and only if the former is recognized as an outlier. An adaptive version of the weighted median filter was specifically proposed for despeckling [54]. Geometric filter (GF) [55] is a powerful tool for edge-preserving smoothing of noise and especially of speckle, the purpose it was designed for.

Anisotropic Diffusion; Refer to [56]-[58]	Anisotropic diffusion 56] is a technique that aims at minimizing noise without eliminating major parts of the image, typically edges and lines or other details that are significant for the image interpretation. The derivation speckle reducing anisotropic diffusion (SRAD) is tailored to coherent images [57]. A notable application of SRAD is for coastline detection in SAR images [58].
Sigma Filter; Refer to [59], [18], [20], [60], [61]	A conceptually simple noise smoothing algorithm is the sigma filter originally developed for additive signal-independent noise [59] and promptly extended to speckle removal [18] also in comparison with local statistics filtering [20]. An enhanced version of Lee's sigma filter [60] is derived and proposed for unbiased filtering of images affected by multiplicative noise with speckle statistics. Eventually, in [61] the bias problem is solved by redefining the sigma range based on the speckle pdf.
Simulated Annealing Despeckling; Refer to [62]-[64]	Simulated Annealing (SA) was originally used for SAR image despeckling and segmentation by White [62]. SA is a stochastic optimization method. Despite its potentiality, the unlikely cartoonlike smoothness produced by SA was noticed in [63]. After that, SA was used only in conjunction with complex multivariate pdf models, like in polarimetric SAR [64].
Bilateral Filtering; Refer to [53], [65]-[67]	The bilateral filter (BF), originally introduced in [65] for grayscale images, has been recently extended to despeckling in [66]. The adaptive method in [67] exploits an order statistic filter, like [53], to reject outliers that often occur. A way to overcome such a drawback is adopting a nonlocal filtering approach.
Nonlocal Filtering; Refer to [68]-[76]	NL filtering is a generalization of the concept of data-driven weighted averaging, in which each pixel is weighted according to its similarity with the reference pixel, as in the pioneering sigma filter [68], [69]. The NL mean filter is extended in the above method [70]-[76].
Total Variation Regularization; Refer to [77]-[84]	Here, denoising is achieved through the minimization of a suitable cost function, combining a data fidelity term with a prior that enforces smoothness while preserving edges [77]. Several solutions exist to apply TV methods in the case of multiplicative noise [78]-[84].
Despeckling Based on Compressed Sensing; Refer to [86]-[88]	Sparse models are at the base of compressed sensing [85], which is the depiction of signals with some samples at a sub-Nyquist rate. Recently, some despeckling methods grounded on the compressed sensing model and sparse illustrations have appeared in [86]–[88].

III. SPECKLE NOISE MODEL

The granular pattern usually found in the Synthetic Aperture Radar (SAR) image either during image acquisition or due to arbitrary constructive or destructive interference is called as speckle noise. Traditional speckle granular pattern appears as in Fig 3. Basically, speckle is not a noise but a scattering phenomenon. However, in the SAR image processing, speckle is modeled as multiplicative noise as shown in equation (3.1).

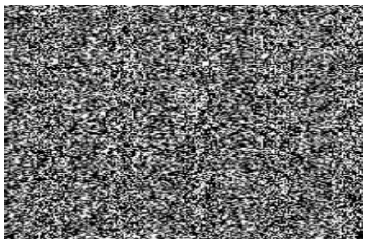

Fig.3 Classical Speckle Pattern

Speckle noise is modeled as multiplicative noise. Therefore the resultant signal is the product of speckle signal and original noise. Let I (i, j) is the degraded pixel of an observed image and S (i, j) be the noise-free image pixel which is to be recovered. With the multiplicative noise model,

$$I(i,j) = S(i,j) * N(i,j) \qquad (3.1)\ [89]$$

In which N (i, j) depicts the multiplicative noise with unit mean and standard deviation [90]. An inherent characteristic of SAR images is the presence of speckle noise. Speckle noise is a random and deterministic in an image. Speckle has a negative impact on SAR images. Radical reduction in contrast resolution may be the main reason for the poor effective resolution.

IV. CONCEPT AND IMPORTANCE OF WAVELET TRANSFORM

A. Wavelet Transform

Wavelets are mostly used in image compression and denoising. DWT delivers the transformation of the image from the spatial to the frequency domain. MATLAB Wavelet Toolbox offers a function, dwt2 for 2D-DWT to analyze the high-frequency component in the image. 2D-

DWT corresponds to multi-resolution approximation expressions. DWT employed using filter bank is shown in Fig 5.

Wavelet is a quickly decaying wave-like oscillation that has zero mean, unlike sinusoidal waves which extend to infinity; a wavelet survives for a finite period. Wavelet comes in different size and shape. Some are Morlet, Daubechies, Coiflets, Bi-orthogonal, Haar, Mexican Hat and Symlets. An availability of wide range of wavelet is the key strength of data analysis. To choose the correct wavelet one needs to consider, the application to use it for, briefly mentioned in Section V.

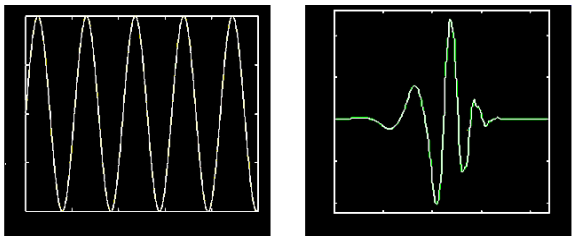

Fig.4 Comparison of Sine Wave and Daubechies 5 Wavelet [91]

In 1976 scientists Croiser, Esteban, and Galand developed a method to decompose the discrete time signals which placed the grounds of DWT. Other researchers named Crochiere, Weber, and Flanagan did the comparable work of coding the speech signals in that year. Their study titled the system as sub-band coding. In 1983, a method related to subband coding was well-defined by Burt and called that method as pyramidal coding which is also recognized as multi-resolution analysis.

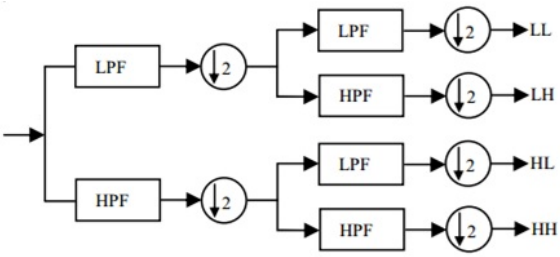

Fig.5 Wavelet Decomposition By Filter banks [92]

A low pass filter and high pass filter are designated in such manner that they accurately halve the frequency range among themselves. This filter pair is recognized as analysis filter pair. To acquire the low-frequency components of the row, the low pass filter is implemented at each row [93]. The low pass filter is half band filter and output data comprise of frequencies in the first half of the original frequency range. Consequently by, Shannon's Sampling Theorem, they can be additionally subsampled by two, so now the resultant data comprises of half of the original number of samples. Now for the same row of data, high pass filter is implemented, and the high-frequency components can be parted similarly and located on the side of low pass components [93]. The method is implemented on all the rows.

Next stage is to implement filtering at every column of the intermediary data. The resultant 2D array of coefficients holds the four bands of data, each written off as LL, HL, LH and HH [93]. To achieve the two level decomposition, the LL band is further decomposed in the same way, thus generating additional sub-bands. This decomposition can be performed up to any level. Thus resultant is pyramidal decomposition as shown below in Fig 6 and 7 [93].

LL: Approximate Image.
LH: Vertical Noisy Coefficients.
HL: Horizontal Noisy Coefficients.
HH: Diagonal Noisy Coefficients.

LL_1	HL_1
LH_1	HH_1

Fig.6 Single level decomposition

<table>
<tr><td>LL_2</td><td>HL_2</td><td rowspan="2">HL_1</td></tr>
<tr><td>LH_2</td><td>HH_2</td></tr>
<tr><td colspan="2">LH_1</td><td>HH_1</td></tr>
</table>

Fig.7 Two level decomposition

Same as the forward transformation to separate the image data into different classes, a reverse transformation is used to reunite the dissimilar classes of data into a restored image. A pair of high and low pass filter is in use here too. Such filter pair is identified as Synthesis Filter pair. This filtering process is just reverse – we initiate from the highest level, implement the filter initially column wise and later row-wise, and likewise, continue to the following level until we reach the first level.

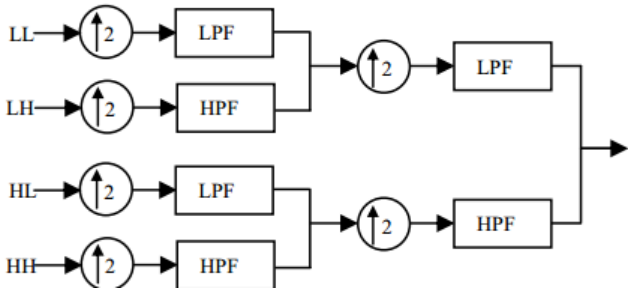

Fig.8 Wavelet Reconstruction Using Filter Banks [92]

B. Wavelet Transform Concepts

1.Scaling

Scaling refers to the process of stretching and shrinking the signal or image in time which can be expressed using below equation.

$$\Psi(t/s)s > 0 \qquad (4.1)$$

where s is a scaling factor which is a positive value and corresponds to how much a signal scaled in time. The scale factor is inversely proportional to frequency.

In wavelet, there is a reciprocal relationship between scale and frequency to the constant of proportionality(COP).

This COP is called as the center frequency of the wavelet because, unlike the sine wave, the wavelet has a bandpass characteristic in the frequency domain. Mathematically the equivalent frequency.

$$F_{eq} = \frac{C_f}{s\,\delta t} \qquad (4.2)$$

C_f is the center frequency of the wavelet; s is the wavelet scale, and δt is the sampling interval. By scaling a wavelet by the factor by 2, it results in reducing the equivalent frequency by an octave.

TABLE II RELATION BETWEEN WAVELET SCALE AND EQUIVALENT FREQUENCY IN THE WAVELET TRANSFORM

Wavelet Scale	2	4	8	16
Equivalent Frequency(F_{eq})	$F_{eq}/2$	$F_{eq}/4$	$F_{eq}/8$	$F_{eq}/16$

A larger scale factor results to the stretched wavelet which corresponds to the lower frequency while small scale factor results to the shrunk wavelet which corresponds to the higher frequency. Hence this helps in capturing the abrupt changes more efficiently. It is possible to construct different scales that inversely correspond to the equivalent frequency as mentioned earlier.

2.Shifting

Shifting a wavelet means delaying and advancing the onset of the wavelet along the length of the signal.

$$Ø(t-k) \qquad (4.3)$$

A shifted wavelet is represented using above notation means; the wavelet is moved and centered at k. Shifting and Scaling process of the DWT is shown in Fig 9.

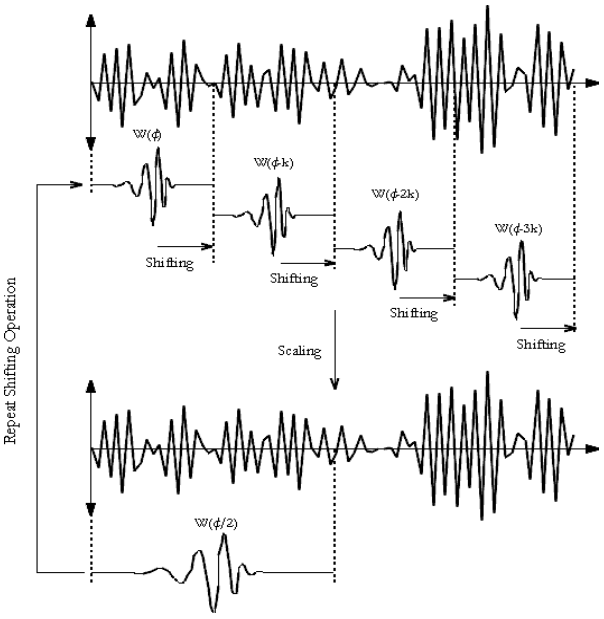

Fig.9 Scaling and Shifting process of DWT

C. Importance

Although the computation of the Continuos Wavelet Transform (CWT) by computers is enabled by the discretized continuous wavelet transform yet it is not considered as a true discrete transform. In reality, the wavelet series is just a sampled version of CWT, and the statistics provided by it are very redundant as far as the restoration of the image is concerned. Due to this redundancy, a significant amount of resources and time is wasted. On the other hand, DWT provides enough information both for analysis and synthesis of the original image, in less computational time.

The DWT is easier and efficient to implement in comparison to CWT. A key application of CWT is time-frequency analysis and filtering of time localized frequency components. A key application of DWT is denoising and compression of signals and images. CWT is used to obtain the simultaneous time and frequency analysis of the signal. Best scale in DWT is sector 2. These two types of wavelet transform differ on how they discretized the scale and translation parameter.

V. DESPECKLING SAR IMAGES USING WAVELET TRANSFORM

A. Wavelet Denoising

This section shows the basic block diagram of wavelet based image denoising and advanced despeckling SAR using wavelet transform. In the basic block diagram i.e. Fig 11, it involves three basic steps- the first step is to compute wavelet transform of the noisy image, the second step is to apply wavelet thresholding on noisy wavelet coefficients using some method, and final step is to apply inverse wavelet transform of modified wavelet coefficients.

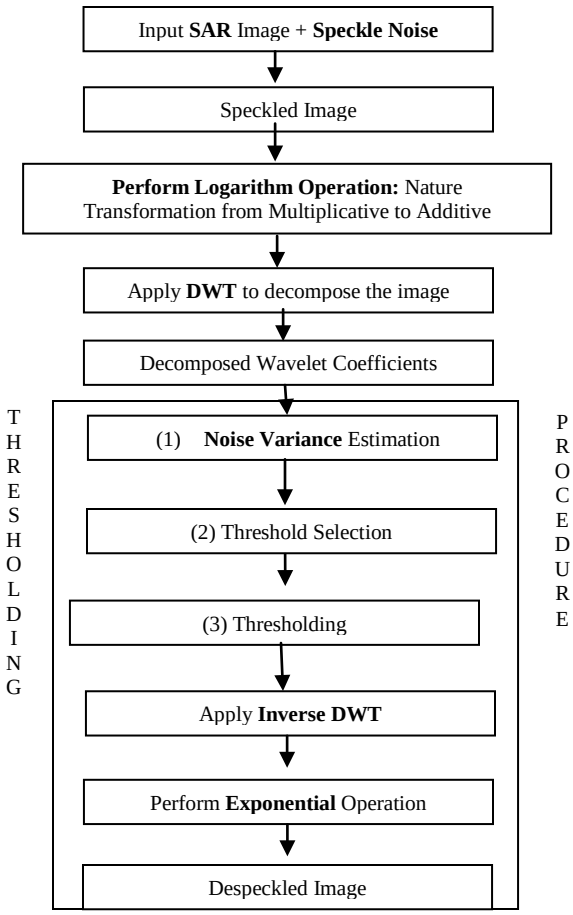

Fig.10 Image Despeckling Procedure [94] [95]

In the detailed despeckling procedure i.e. Fig 10, firstly speckle noise is added to the original SAR image, as SAR image is multiplicative in nature which increases the computational time of the despeckling process, so its transformation from multiplicative to additive nature is required which reduces the computational time. To perform such operation, logarithm operation is performed. This log transformation changes its nature from multiplicative to additive which helps to use additive noise model in a more appropriate way. Later on, wavelet transformation is applied. It has following steps.

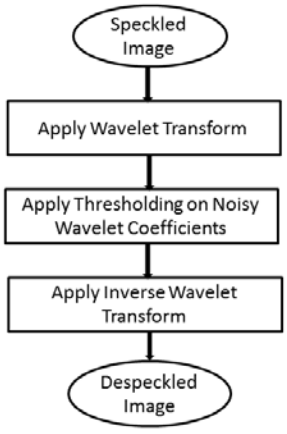

Fig.11 Basic Block Diagram of Wavelet-Based Denoising

B. Wavelet Shrinkage

Wavelet shrinkage is the mainly responsible for despeckling, which involves mainly two steps, threshold selection, and thresholding method.

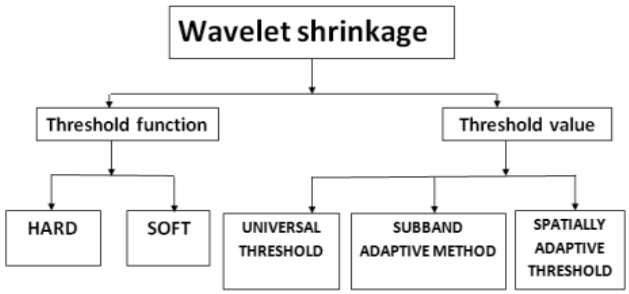

Fig.12 Block diagram of threshold process and its different methods [96]

The despeckling algorithm selects the optimal threshold value, and this threshold value can be applied in three ways mentioned above in Fig 12.

1. Thresholding Value

Selecting a threshold value is an important and critical task in wavelet denoising method as this threshold value plays a major role in separating the noisy coefficients from the detail coefficients as detail coefficients are useful for the restoration of the image. Threshold selection method involves three categories: Universal threshold, Subband adaptive threshold and spatially adaptive threshold. In universal threshold, the threshold value is uniquely chosen for all wavelet coefficients [5], [96]. In sub-band adaptive thresholding, the threshold value is selected separately for each detail sub-band [96], [97]. In spatially adaptive threshold way, each detailed wavelet coefficient has its own threshold value [96]-[98].

2. Wavelet Thresholding

Generally, in wavelet denoising, it is considered that details of the image are preserved by the low threshold value, but this small threshold is inefficient to remove the noise, but a large threshold value removes the noise efficiently, but it destroys the detail portion. These drawbacks are overcome by the different thresholding rules which are mentioned in the literature. Standard methods are summarized below.

VisuShrink: This method was originated by Donoho and Johnstone [99], [100] and it applies the universal threshold; it works on the use of a fixed (or universal) threshold described by the below equation:

$$T_u = \sigma_n^2 \sqrt{2 \log N} \qquad (5.1)$$

VisuShrink is a general threshold selector method that takes image size (N) and the noise standard deviation σ_n into

account; though it reduces the maximum error overall number of pixels in the image it produces an overly smoothed approximation that is mismatched to discontinuities in the signal, introducing artifacts in the images [101], [102]. An estimate of the noise level σ_n in (5.1) is grounded on the median absolute deviation given by [103] in the equation 5.2.

$$\sigma_n^2 = \left[\frac{median(HH1(n,m))}{0.6745}\right]^2 \qquad (5.2)$$

where n and m represent the pixel indexes of the diagonal sub-band of the first level wavelet decomposition of the image i.e. HH1. The selected universal threshold is not adaptive to the image as it does not take image properties into account. For 512*512 dimension size images or greater size, then the selected universal threshold can be excessively large due to its direct link with N in equation 5.1. This creates overly smoothed image that eliminates many coefficients.

SureShrink: This technique combines both Stein's unbiased risk estimator (SURE) technique and universal threshold [103]. Here a unique threshold is computed for each sub-band which is suited for SAR images with sharp discontinuities; this technique shows good despeckling performance and assures small values of the mean square error [101]. Here, the soft threshold is formulated as,

$$T_S = min\left(T, \sigma_n^2\sqrt{2logN}\right) \qquad (5.3)$$

here T represents the value that minimizes the SURE.

BayesShrink: It is a technique grounded on the hypothesis that the wavelet coefficients are demonstrated as random variables with general Gaussian distribution (GGD) within each sub-band. Under this condition, in order to minimize the Bayesian risk, the value is find using estimated threshold [101], [34].

$$T_B(\sigma_x) = \frac{\sigma_n^2}{\sigma_x} \qquad (5.4)$$

where σ_x is the standard deviation of image computed at each wavelet sub-band.

Implementation wise, BayesShrink and SureShrink works in the same manner, but BayesShrink shows better results when GGD is assumed [103]. This threshold adapts both image and noise properties. But in the case of SAR images, the noise is multiplicative in nature [6], so the previously mentioned thresholding techniques cannot be directly implemented to the speckled image. To deal with such situation, a preprocessing step is required like log transformation which can transform the multiplicative nature of the speckle noise into additive, which is explained in the next section.

Another important aspect in coefficients processing is the thresholding operation, which describes the method used to distinguish between the detail and noisy coefficients. There are two methods used for the thresholding process [104], described below:

Hard thresholding: Hard thresholding sets any coefficient less than or equal to the threshold to zero [105].

```
if (coef[i] <= thresh)
coef[i] = 0.0;
```

Soft thresholding: Hard thresholding adjusts coefficient less than or equal to the threshold to zero [105]. The threshold is deducted from that coefficient that is larger than the threshold. This moves the time series toward zero [105].

```
if (coef[i] <= thresh)
coef[i] = 0.0;
else
coef[i] = coef[i] - thresh;
```

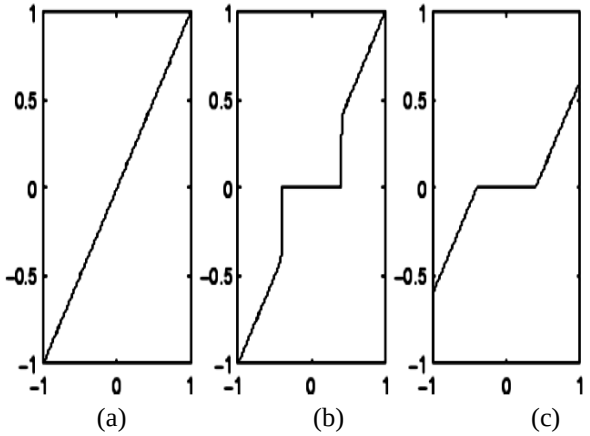

Fig.13 (a) Original Signal (b) Hard Threshold Signal (c) Soft Threshold Signal [106]

C. Wavelet Families

The Wavelet Toolbox™ software contains wavelet family which includes a large number of wavelets that can be used for both continuous and discrete analysis. Various wavelet family members are 'haar'-Haar wavelet, 'db'-Daubechies wavelets, 'sym'-Symlets, 'coif'-Coiflets, 'bior'-Biorthogonal wavelets, 'rbio'-Reverse biorthogonal wavelets, etc. [107]. In this paper, results are presented using Daubechies wavelets as Daubechies wavelets are the most admired wavelets [108]. Also, Haar, Daubechies, Symlets and Coiflets supported orthogonal wavelets compactly [109]. Haar is the first and simplest: a step function, Ingrid Daubechies invented the compactly supported orthonormal wavelets, making DWT practicable; Biorthogonal exhibits the linear phase property, needed for signal (and image) reconstruction [110].

D. Logarithmic Transformation

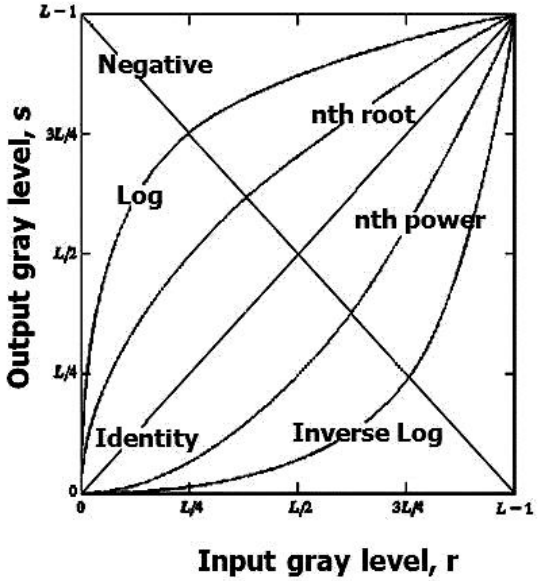

Fig.14 Gray-level transformation operations used for image enhancement [109]

The log transformation curvature is presented in Fig 14. Log transformation of the image is equated as 5.1.

$$s = c^* \log (1 + r) \qquad (5.1)$$

Here, c is constant, and it is assumed that r≥0. r is a pixel value of input image, and s is a pixel value of output image. The value one is added in case the input pixel value is 0, then log(0) becomes infinity. So one is to be added to handle such situation and to make the minimum value at least 1. The value of c in log transform is adjusted according to the need of enhancement required by the researcher.

Let p and q represent speckled SAR image and the corresponding speckle free SAR image respectively. Let say n_{mul} depicts multiplicative speckle noise component. Then, according to multiplicative noise model,

$$p = q * n_{mul} \qquad (5.2)$$

It is hard to know the actual statistics behind the speckle noise as it involves complex analytical and conceptual models. Therefore transformation from multiplicative noise model to additive is performed by log transform on speckled SAR image.

$$\log(p) = \log(q) + \log(n_{mul}) \qquad (5.3)$$

$$p' = q' + n' \qquad (5.4)$$

p', q' and n' shows the log of the quantities in equation 5.2 and now n' is signal independent as log transform removes the signal dependency of the speckle noise.

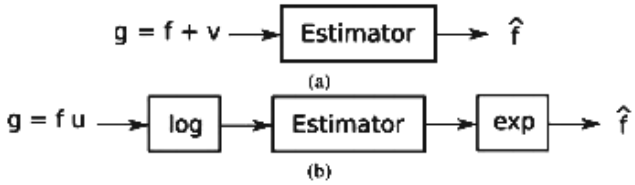

Fig.15 Additive models used in despeckling algorithms [103]: (a) signal-dependent in the spatial domain; (b) signal-independent in the spatial domain.

VI. EXPERIMENTAL TEST RESULTS AND ANALYSIS

This section shows the resultant images of speckled SAR images and log transformed speckled SAR image on applying DWT with the first, second and third level of decomposition. These experimental results will show the difference of implementing the DWT on the quality parameter of speckled SAR image and log transformed speckled SAR image [111] regarding its effects on the texture part. As DWT on being applied generates a large number of small coefficients and a small number of large coefficients. The results are presented using the image shown in Fig 1.

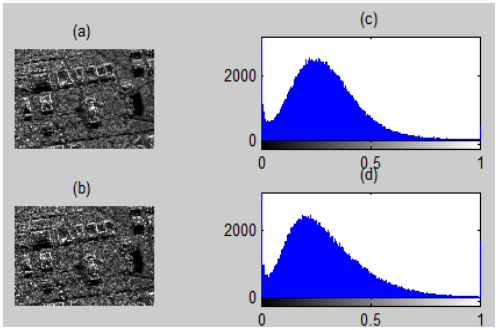

Fig.16 (a) Original SAR Image (b) Speckled SAR Image (Speckle Noise: 7%) (c) Histogram of Original SAR Image (d) Histogram of Speckled SAR Image. [111]

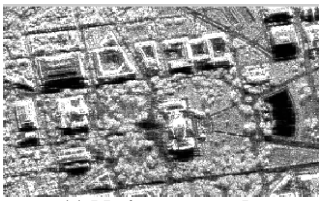

(a) LL-Approximate Image

(b) LH-Horizontal detail

(c) HL-Vertical Detail

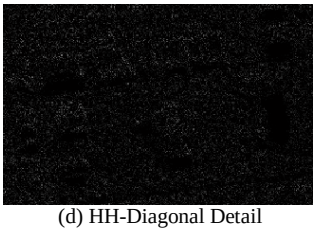

(d) HH-Diagonal Detail

Fig.17 First Level of decomposition on Speckled Image

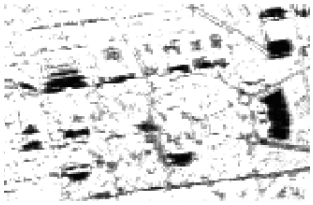

(a) LL-Approximate Image

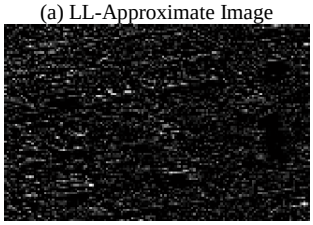

(b) LH-Horizontal detail

(c) HL-Vertical Detail

(d) HH-Diagonal Detail

Fig.18 Second Level of decomposition on Speckled Image

(a) LL-Approximate Image

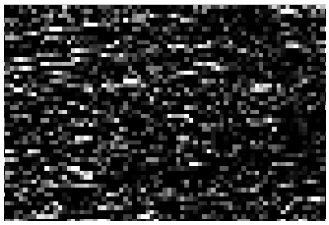

(b) LH-Horizontal detail

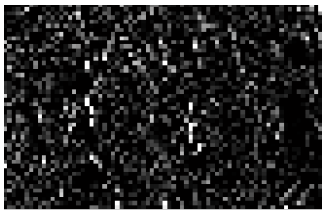

(c) HL-Vertical Detail

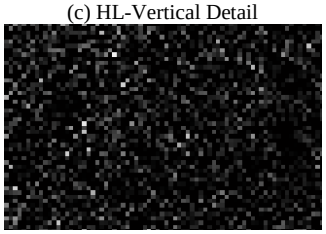

(d) HH-Diagonal Detail

Fig 19 Third Level of decomposition on Speckled Image

Fig 16, 17, 18 and 19 shows the change in the statistical properties of the speckled SAR image while applying DWT. Next figures will show the results of the implementation of the DWT on the log transformed speckled SAR image [111]. All the four sub-bands are shown. It can be easily seen and analyzed that although log transformation helps in implementing additive noise models but still it degrades the quality of the SAR image although its effects can be restored using exponent operation.

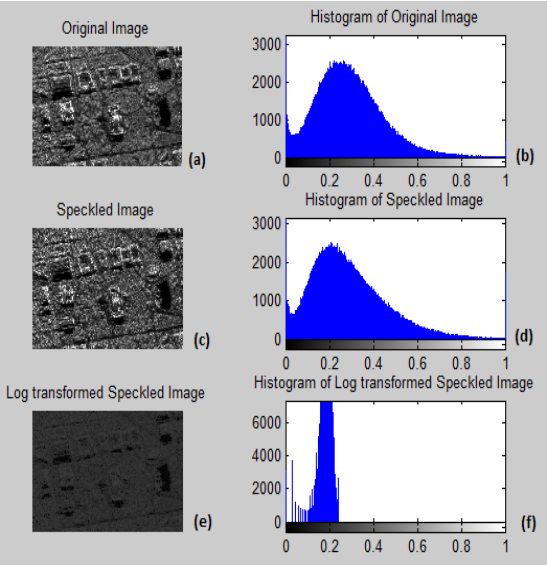

Fig.20. (a) Original SAR Image (b) Histogram of Original SAR Image (c) Speckled Image (d) Histogram of Speckled SAR Image (e) Log Transformed Speckled Image (f) Histogram of Log Transformed Speckled Image [111].

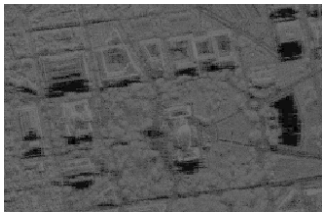

(a) LL-Approximate Image

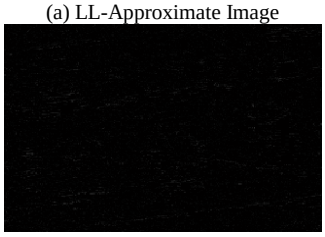

(b) LH-Horizontal detail

(c) HL-Vertical Detail

(d) HH-Diagonal Detail

Fig.21 First Level of decomposition on Log Transformed Speckled Image

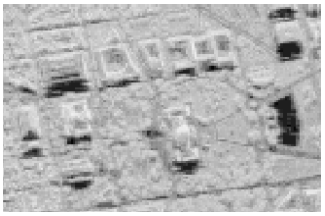

(a) LL-Approximate Image

(b) LH-Horizontal detail

(c) HL-Vertical Detail

(d) HH-Diagonal Detail

Fig.22 Second Level of decomposition on Log Transformed Speckled Image

(a) LL-Approximate Image

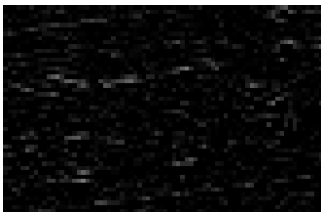

(b) LH-Horizontal detail

(c) HL-Vertical Detail

(d) HH-Diagonal Detail

Fig.23 Third Level of decomposition on Log Transformed Speckled Image

Fig 20, 21, 22 and 23 shows the various sub-band of the log transformed speckled image at first, the second and third level of decomposition. On performing a comparative analysis, it can be easily seen and verified that DWT on log transformed speckled image generates a more large number of small coefficients and a small number of large coefficients than speckled image. This qualitative analysis shows that the operation of log transformation degrades the quality of SAR image, but still, it is in use due to its transformation nature as it changes the multiplicative nature of the speckle noise to the additive. Due to which all the easily available additive noise restoration models can be used and applied on the log transformed speckled image.

TABLE III COMPARISON OF SPECKLED IMAGE WITH LOG TRANSFORMED SPECKLED IMAGE

Speckle Noise v(p)	s=c*log (1+r)	Speckled Image		Log Transformed Speckled Image	
		SNR	PSNR	SNR	PSNR
0.04(4%)	c=0.1	14.0342	22.1004	4.9913	13.0516
0.1(10%)	c=0.1	10.1175	18.1837	4.9287	12.9950
0.2(20%)	c=0.1	7.2147	15.2809	4.7943	12.8605
0.3(30%)	c=0.1	5.5706	13.6368	4.5631	12.6293
0.4(40%)	c=0.1	4.4740	12.5402	4.2566	12.3228
0.5(50%)	c=0.1	3.7582	11.8244	4.0485	12.1147
0.6(60%)	c=0.1	3.2600	11.3262	3.9012	11.9675

v = variance of speckle noise, p = percentage of speckle noise, s = pixel value of output image, r = pixel value of input image, c = constant, SNR = Signal to Noise Ratio, PSNR = Peak Signal to Noise Ratio

Table III demonstrates the effect of applying log transformation on the speckled image using performance metrics i.e. SNR and PSNR. As it can be noticed in Fig 16 and 20 that as log transform is applied in Fig 20, the amount of dark pixels is increased and light pixels is reduced. It can be easily seen and validated through table iii that the quality of the log transformed speckled image gets poorer as comparison to the speckled image. The SNR and PSNR of log transformed speckled image is reduced as comparative to speckled image. This indicates the quality degradation. This degradation does not conclude that log transformation is not a legitimate operation. It only shows that speckle noise is multiplicative in nature and log transform is applied to change its nature form multiplicative to additive. Although its implementation degrades the quality of the image but it also resolves the problem of using additive noise models on speckle image. Graphs in fig 24 and 25 shows the effect of adding speckle noise in SAR image and log transformed image.

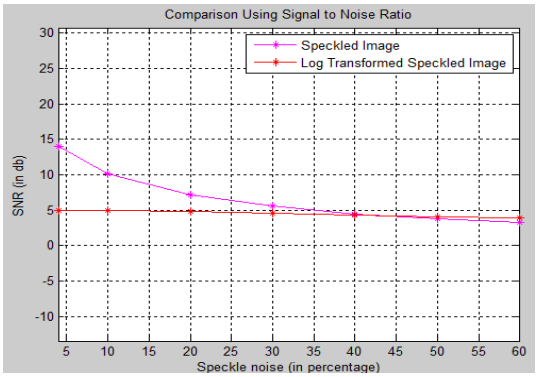

Fig.24 Comparative analysis of Speckled Image with Log Transformed Speckled Image Using SNR

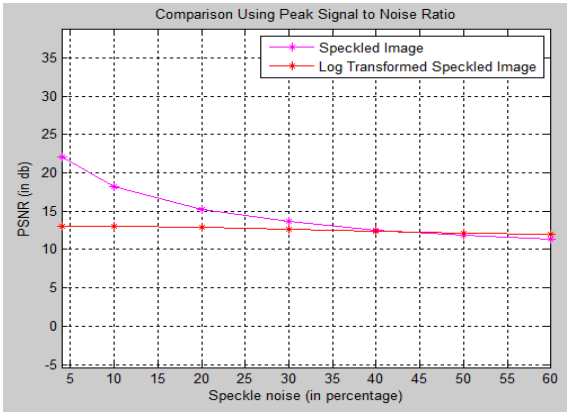

Fig.25 Comparative analysis of Speckled Image with Log Transformed Speckled Image Using PSNR

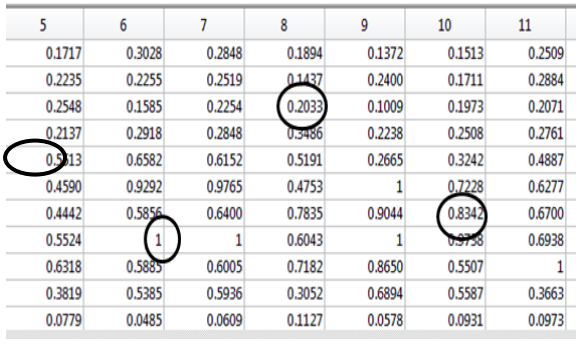

5	6	7	8	9	10	11
0.1717	0.3028	0.2848	0.1894	0.1372	0.1513	0.2509
0.2235	0.2255	0.2519	0.1437	0.2400	0.1711	0.2884
0.2548	0.1585	0.2254	0.2033	0.1009	0.1973	0.2071
0.2137	0.2918	0.2848	0.3486	0.2238	0.2508	0.2761
0.5313	0.6582	0.6152	0.5191	0.2665	0.3242	0.4887
0.4590	0.9292	0.9765	0.4753	1	0.7228	0.6277
0.4442	0.5856	0.6400	0.7835	0.9044	0.8342	0.6700
0.5524	1	1	0.6043	1	0.9758	0.6938
0.6318	0.5885	0.6005	0.7182	0.8650	0.5507	1
0.3819	0.5385	0.5936	0.3052	0.6894	0.5587	0.3663
0.0779	0.0485	0.0609	0.1127	0.0578	0.0931	0.0973

Fig.26 Snapshot of Coefficient Band of Speckled Image before Applying Log Transformation

Fig 26 shows the coefficient summary of the speckled image. It can easily analyzed in the coefficient band that coefficient varies from 0 to 1, which depicts that image has

black, white and gray portion. Those coefficients that are close to 0 and 1 are major parts that are seriously affected by the speckle noise. Log transform is applied to each can every pixel one by one. This operation results in the reduction of the pixel values of all the dark, bright and gray pixels. Log transform provides uniformity in the image which later helps in restoration process. The results of the log transformation are validated below. Since this operation is performed over each and every pixel. For an instance, three pixels are selected as shown in the Fig 26 for validation.

For pixel value = 1; value of constant (c) is 0.1 for all cases.

$$s = c * \log (1+r)$$
$$s = 0.1 * \log (1+1)$$
$$s = 0.1 * \log (2)$$
$$s = 0.1 * 0.30103$$
$$s = 0.030103$$

For pixel value = 0.2033;

$$s = c * \log (1+r)$$
$$s = 0.1 * \log (1+0.2033)$$
$$s = 0.1 * \log (1.2033)$$
$$s = 0.1 * 0.08038$$
$$s = 0.00804$$

For pixel value = 0.8342;

$$s = c * \log (1+r)$$
$$s = 0.1 * \log (1+0.8342)$$
$$s = 0.1 * \log (1.8342)$$
$$s = 0.1 * 0.26345$$
$$s = 0.02635$$

For pixel value = 0.5513;

$$s = c * \log (1+r)$$
$$s = 0.1 * \log (1+0.5513)$$
$$s = 0.1 * \log (1.5513)$$
$$s = 0.1 * 0.19070$$
$$s = 0.01907$$

Let if pixel value = 0;

$$s = c * \log (1+r)$$
$$s = 0.1 * \log (1+0)$$
$$s = 0.1 * \log (1)$$
$$s = 0.1 * 0$$
$$s = 0$$

It can be easily verified that how log transform affects the speckled image. It degrades the quality of the SAR image, as after its implementation it can be seen in all the above five cases that the pixel values tend towards 0 resulting to a darker image. Regardless this drawback, it provides the uniformity in the image which later helps to the additive noise models in the process of the image despeckling.

VII. CONCLUSION

This research paper is written with the vision to answer the basic doubts of the researchers who wants to work in the field of despeckling SAR images using wavelet domain. This article focuses on the core concept of DWT including its role, importance and implementation. It further discusses and analyses the DWT implementation on the speckled image and log transformed speckled image up to three levels of decomposition. Log transform is applied to convert the multiplicative nature of the speckle noise into additive. This operation degrades the quality of the images, but still is in use, as the available additive noise restoration models can be utilized easily to despeckle SAR images. This paper also discusses the detailed analysis of SAR image using wavelet transform and various aspects of log transformation. The paper concludes with the idea that DWT degrades the log transformed speckled image more than the speckled image, as various sub-bands of log transformed speckled image generates a more large number of small coefficients and a smaller number of large coefficients which indicates more distortion.

REFERENCES

[1] SAR Image Processing, Sandia National Laboratories (Synthetic Aperture Radar Imagery Database), Available: http://www.sandia.gov/RADAR/imagery/index.html#tab-2

[2] Mathswork Matlab Youtube Channel, Understanding Wavelets video, Understanding Wavelets, Part 1: What Are Wavelets, Available: https://www.youtube.com/watch?v=QX1-xGVFqmw?

[3] D.T.Kuan *et al*., "Adaptive restoration of images with speckle", *IEEE Trans. Acc. Speech and signal Proc.*, Vol. 35, No.3, pp.373-383, March 1987.

[4] Tinku Acharya and Ajoy K. Ray, *Image Processing Principles and Application*s, edition A John Wiley & Sons, Mc., Publication, 2005.

[5] J.S.Lee, "Digital image enhancement and noise filtering by use of local statistics*", IEEE Trans. On Pattern Analysis and Matching Intelligence*, vol. PAMI-2, pp.165-168, 1980.

[6] Anil K.Jain, *Fundamentals of Digital Image Processing*, first edition, Prentice – Hall, Inc., 1989.

[7] V.S.Frost *et al*, "A model for radar images and its application to adaptive digital filtering of multiplicative noise*", IEEE Trans. Pattern Anal. And Machine Intell.*,vol. PAMI-4, pp.157-166. 1982.

[8] DT Kuan ,AA Sawchuk , TC Strand and P. Chavel , "Adaptive noise smoothing filter for images with signal dependent noise", *IEEE Trans Pattern Anal Mach Intell.*; PAMI-7(2):165–77, Mar 1985.

[9] L Gagnon ,A. Jouan , "Speckle filtering of SAR images – a comparative study between a complex-wavelet-based and standard filter", *Proc SPIE;* pp. 80–91, 1997.

[10] M. Dai ,C. Peng ,AK. Chan ,D. Loguinov and Bayesian , "wavelet shrinkage with edge detection for SAR image de-speckling", *IEEE Trans Geo Sci Remote Sens.,* Vol.42,No. 8,pp.1642–1648, Aug 2004.

[11] A. Achim ,EE. Kuruoglu and J. Zerubia, "SAR image filtering based on the heavy-tailed Rayleigh model," *IEEE Trans Image Process.*,Vol.15,No.9, pp.2686–93. Sep. 2006.

[12] T. Bianchi ,F. Argenti and L. Alparone , "Segmentation-based map despeckling of SAR images in the undecimated wavelet domain," *IEEE Trans Geoscience and Remote Sensing, Vol.* 46, No.9, pp. 2728–42, 2008.

[13] J Wu ,W. Yan , H. Bian , and Ni W, "A despeckling algorithm combining curvelet and wavelet transforms of high resolution SAR images," *Proc Computer Design and Applications,* Vol.1, pp.302–5, June 2010.

[14] C Jojy , Nair MS, Subrahmaniyam GRKS and R Riji, "Discontinuity adaptive non-local means with importance sampling unsented Kalman filter for despeckling SA images," *IEEE Transaction on selected topics in Applied Earth Observation And Remote Sensing*,Vol. 6, No.4, Aug 2013.

[15] Abdourrahmane Mahamane Atto, Emmanuel Trouvé, Jean-Marie Nicolas, and Thu Trang Lê, "Wavelet Operators and Multiplicative Observation Models—Application to SAR Image Time-Series Analysis", *IEEE Transactions On Geoscience And Remote Sensing*, Vol. 54, No. 11, November 2016.

[16] Diego Gragnaniello, Giovanni Poggi, Giuseppe Scarpa, and Luisa Verdoliva, "SAR Image Despeckling by Soft Classification," Published in: *IEEE Journal of Selected Topics in Applied Earth Observations and Remote Sensing* (Volume: 9, Issue: 6, June 2016), Page(s): pp.2118 – 2130, Date of Publication: 27 May 2016.

[17] Fabrizio argenti, alessandro lapini, and luciano alparone, "A Tutorial on Speckle Reduction in Synthetic Aperture Radar Images," IEEE Geoscience and remote sensing magazine September 2013.

[18] J.S. Lee, "Digital image smoothing and the sigma filter," Comput. Vis. Graph. Image Process., vol. 24, No. 2, pp. 255–269, Nov. 1983.

[19] J.S. Lee, "Speckle analysis and smoothing of synthetic aperture radar images," Comput. Graph. Image Process., vol. 17, No. 1, pp. 24–32, Sept. 1981.

[20] J.S. Lee, "Speckle suppression and analysis for synthetic aperture radar images," Opt. Eng., vol. 25, no. 5, pp. 636–643, May 1986.

[21] J.-S. Lee, "Refined filtering of image noise using local statistics," Comput. Graph. Image Process., vol. 15, No. 2, pp. 380–389, Apr. 1981.

[22] B. Aiazzi, L. Alparone, S. Baronti, and A. Garzelli, "Coherence estimation from incoherent multi look SAR imagery," *IEEE Trans. Geosci. Remote Sensing*, vol. 41, No. 11, pp. 2531–2539, Nov. 2003.

[23] A. Lopès, E. Nezry, R. Touzi, and H. Laur, "Maximum a posteriori speckle filtering and first order texture models in SAR images," in Proc. *IEEE Int. Geoscience and Remote Sensing Symp. (IGARSS)*, pp. 2409–2412, 1990.

[24] A. Lopès, E. Nezry, R. Touzi, and H. Laur, "Structure detection and statistical adaptive speckle filtering in SAR images," *Int. J. Remote Sensing*, vol. 14, No. 9, pp. 1735–1758, June 1993.

[25] A. Baraldi and F. Parmiggiani, "A refined gamma MAP SAR speckle filter with improved geometrical adaptivity," *IEEE Trans. Geosci. Remote Sensing*, vol. 33, No. 6, pp. 1245–1257, Nov. 1995.

[26] M. Walessa and M. Datcu, "Model-based despeckling and information extraction from SAR images," *IEEE Trans. Geosci. Remote Sensing*, vol. 38, No. 5, pp. 2258–2269, Sept. 2000.

[27] D. E. Molina, D. Gleich, and M. Datcu, "Evaluation of Bayesian despeckling and texture extraction methods based on Gauss–Markov and auto-binomial Gibbs random fields: Application to TerraSAR-X data," *IEEE Trans. Geosci. Remote Sensing*, Vol. 50, No. 5, pp. 2001–2025, May 2012.

[28] A. Lopès, R. Touzi, and E. Nezry, "Adaptive speckle filters and scene heterogeneity," *IEEE Trans. Geosci. Remote Sensing*, Vol. 28, No. 6, pp. 992–1000, Nov. 1990.

[29] P. Meer, R.-H. Park, and K. Cho, "Multiresolution adaptive image smoothing," *Graph. Models Image Process.*, Vol. 56, No. 2, pp. 140–148, Mar. 1994.

[30] B. Aiazzi, L. Alparone, and S. Baronti, "Multiresolution local-statistics speckle filtering based on a ratio Laplacian pyramid," *IEEE Trans. Geosci. Remote Sensing*, Vol. 36, No. 5, pp. 1466–1476, Sept. 1998.

[31] B. Aiazzi, L. Alparone, S. Baronti, and G. Borri, "Pyramid-based multiresolution adaptive filters for additive and multiplicative image noise," *IEEE Trans. Circuits Syst. II*, Vol. 45, No. 8, pp. 1092–1097, Aug. 1998.

[32] B. Aiazzi, L. Alparone, S. Baronti, and F. Lotti, "Lossless image compression by quantization feedback in a content-driven enhanced Laplacian pyramid," *IEEE Trans. Image Process.*, Vol. 6, No. 6, pp. 831–843, June 1997.

[33] B. Aiazzi, L. Alparone, S. Baronti, G. Chirò, F. Lotti, and M. Moroni, "A pyramid-based error-bounded encoder: An evaluation on X-ray chest images," *Signal Process*., Vol. 59, No. 2, pp. 173–187, June 1997.

[34] D. L. Donoho, "De-noising by soft-thresholding," *IEEE Trans. Inform*. Theor.,Vol. 41, No. 3, pp. 613–627, May 1995.

[35] L. Gagnon and A. Jouan, "Speckle filtering of SAR images: A comparative study between complex-wavelet-based and standard filters," *in Proc. SPIE, Wavelet Applications in Signal and Image processing V*, Vol. 3169, pp. 80–91, 1997.

[36] E. Hervet, R. Fjørtoft, P. Marthon, and A. Lopès, "Comparison of wavelet-based and statistical speckle filters," *in Proc. SPIE SAR Image Analysis, Modelling, and Techniques III*, F. Posa, Ed., Vol. 3497, pp. 43–54, 1998.

[37] M. Simard, G. DeGrandi, K. P. B. Thomson, and G. B. Bénié, "Analysis of speckle noise contribution on wavelet decomposition of SAR images," *IEEE Trans. Geosci. Remote Sensing*, Vol. 36, No. 6, pp. 1953–1962, Nov. 1998.

[38] H. Guo, J. E. Odegard, M. Lang, R. A. Gopinath, I. W. Selesnick, and C. S. Burrus, "Wavelet-based speckle reduction with application to SAR based ATD/R," *in Proc. IEEE Int. Conf. Image Processing (ICIP)*, 1994, Vol. 1, pp. 75–79.

[39] J. R. Sveinsson and J. A. Benediktsson, "Almost translation invariant wavelet transformations for speckle reduction of SAR images," *IEEE Trans. Geosci. Remote Sensing*, Vol. 41, No. 510, pp. 2404–2408, Oct. 2003.

[40] S. Foucher, G. B. Bénié, and J.-M. Boucher, "Multiscale MAP filtering of SAR images," *IEEE Trans. Image Process.*, Vol. 10, No. 1, pp. 49–60, Jan. 2001.

[41] F. Argenti and L. Alparone, "Speckle removal from SAR images in the undecimated wavelet domain," *IEEE Trans. Geosci. Remote Sensing*, Vol. 40, No. 11, pp. 2363–2374, Nov. 2002.

[42] M. Dai, C. Peng, A. K. Chan, and D. Loguinov, "Bayesian wavelet shrinkage with edge detection for SAR image despeckling," *IEEE Trans. Geosci. Remote Sensing*, Vol. 42, No. 8, pp. 1642–1648, Aug. 2004.

[43] R. Touzi, A. Lopès, and P. Bousquet, "A statistical and geometrical edge detector for SAR images," *IEEE Trans. Geosci. Remote Sensing*, Vol. 26, No. 6, pp. 764–773, Nov. 1988.

[44] S. Solbø and T. Eltoft, "C-WMAP: A statistical speckle filter operating in the wavelet domain," *Int. J. Remote Sens*., Vol. 25, No. 5, pp. 1019–1036, Mar. 2004.

[45] F. Argenti, T. Bianchi, and L. Alparone, "Multiresolution MAP despeckling of SAR images based on locally adaptive generalized Gaussian PDF modeling," *IEEE Trans. Image Process.*, Vol. 15, No. 11, pp. 3385–3399, Nov. 2006

[46] R. Tao, H. Wan, and Y. Wang, "Artifact-free despeckling of SAR images using contourlet," *IEEE Geosci. Remote Sensing Lett.*, Vol. 9, No. 5, pp. 980–984, Sept. 2012.

[47] F. Argenti, T. Bianchi, A. Lapini, and L. Alparone, "Fast MAP despeckling based on Laplacian–Gaussian modeling of wavelet coefficients," *IEEE Geosci. Remote Sensing Lett.*, Vol. 9, No. 1, pp. 13–17, Jan. 2012.

[48] H. Chen, Y. Zhang, H. Wang, and C. Ding, "Stationary-wavelet based despeckling of SAR images using two-sided generalized gamma models," *IEEE Geosci. Remote Sensing Lett.*, 1998, Vol. 9, No. 6, pp. 1061–1065, Nov. 2012.

[49] H.-C. Li, W. Hong, Y.-R. Wu, and P.-Z. Fan, "Bayesian wavelet shrinkage with heterogeneity-adaptive threshold for SAR image despeckling based on generalized gamma distribution," *IEEE Trans. Geosci. Remote Sensing*, Vol. 51, No. 4, pp. 2388– 2402, Apr. 2013.

[50] A. Pižurica, W. Philips, I. Lemahieu, and M. Acheroy, "A versatile wavelet domain noise filtration technique for medical imaging," *IEEE Trans. Med. Imag*., Vol. 22, No. 3, pp. 323–331, Mar. 2003.

[51] S. Fukuda and H. Hirosawa, "Smoothing effect of wavelet based speckle filtering: The Haar basis case," *IEEE Trans. Geosci. Remote Sensing*, Vol. 37, No. 2, pp. 1168–1172, Mar. 1999.

[52] Y. Hawwar and A. Reza, "Spatially adaptive multiplicative noise image denoising technique," *IEEE Trans. Image Process*., Vol. 11, No. 12, pp. 1397–1404, Dec. 2002.

[53] L. Alparone, S. Baronti, and R. Carlà, "Two-dimensional rank conditioned median filter," *IEEE Trans. Circuits Syst. II*, Vol. 42, No. 2, pp. 130–132, Feb. 1995.

[54] L. Alparone, S. Baronti, R. Carlà, and C. Puglisi, "An adaptive order-statistics filter for SAR images," *Int. J. Remote Sens.*, Vol. 17, No. 7, pp. 1357–1365, May 1996.

[55] T. R. Crimmins, "Geometric filter for speckle reduction," Appl. Opt., Vol. 24, No. 10, pp. 1438–1443, May 1985.

[56] P. Peronaand and J. Malik, "Scale-space and edge detection using anisotropic diffusion," *IEEE Trans. Pattern Anal. Mach. Intell.*, Vol. 12, No. 7, pp. 629–639, July 1990.

[57] Y. Yuand S. T. Acton, "Speckle reducing anisotropic diffusion," *IEEE Trans. Image Process.*, Vol. 11, No. 11, pp. 1260–1270, Nov. 2002.

[58] Y. Yu and S. T. Acton, "Automated delineation of coastline from polarimetric SAR imagery," *Int. J. Remote Sens.*, Vol. 25, No. 17, pp. 3423–3438, Sept. 2004.

[59] J.-S. Lee, "Digital image smoothing and the sigma filter," *Comput. Vis. Graph. Image Process.*, Vol. 24, No. 2, pp. 255–269, Nov. 1983.

[60] L. Alparone, S. Baronti, and A. Garzelli, "A hybrid sigma filter for unbiased and edge-preserving speckle reduction," in Proc. *IEEE Int. Geoscience and Remote Sensing Symp. (IGARSS)*, Vol. 2, pp. 1409–1411, 1995.

[61] L. Alparone, S. Baronti, and A. Garzelli, "A hybrid sigma filter for unbiased and edge-preserving speckle reduction," in Proc. *IEEE Int. Geoscience and Remote Sensing Symp. (IGARSS)*, Vol. 2, pp. 1409–1411, 1995.

[62] R. G. White, "A simulated annealing algorithm for SAR and MTI image cross-section estimation," *in Proc. SPIE SAR Data Processing for Remote Sensing 137*, 1994, Vol. 2316, pp. 339–360.

[63] I. McConnelland and C. Oliver, "Comparison of annealing and iterated filters for speckle reduction in SAR," *in Proc. SPIE Microwave Sensing and Synthetic Aperture Radar 74*, 1994, Vol. 2958, pp. 74–85.

[64] J. Schouand and H. Skriver, "Restoration of polarimetric SAR images using simulated annealing," *IEEE Trans. Geosci. Remote Sensing*, Vol. 39, No. 9, pp. 2005–2016, Sept. 2001.

[65] C. Tomasiand and R. Manduchi, "Bilateral filtering for gray and color images," *in Proc. 6th Int. Conf. Computer Vision (ICCV)*, 1998, pp. 839–846.

[66] W. G. Zhang, Q. Zhang, and C. S. Yang, "Improved bilateral filtering for SAR image despeckling," *Electron. Lett.*, Vol. 47, No. 4, pp. 286–288, Feb. 2011.

[67] G.T. Li, C.-L. Wang, P.- P. Huang and W.-D. Yu, "SAR image despeckling using a space-domain filter with alterable window," *IEEE Geosci. Remote Sensing Lett.*, Vol. 10, No. 2, pp. 263–267, Mar. 2013.

[68] C.A. Deledalle, L. Denis, and F. Tupin, "Iterative weighted maximum likelihood denoising with probabilistic patch based weights," *IEEE Trans. Image Process.*, Vol. 18, No. 12, pp. 2661–2672, Dec. 2009.

[69] S. Parrilli, M. Poderico, C. V. Angelino, and L. Verdoliva, "A nonlocal SAR image denoising algorithm based on LLMMSE wavelet shrinkage," *IEEE Trans. Geosci. Remote Sensing*, Vol. 50, No. 2, pp. 606–616, Feb. 2012.

[70] A. Buades, B. Coll, and J.-M. Morel, "A non-local algorithm for image denoising," *in Proc. IEEE Conf. Computer Vision and Pattern Recognition (ICCVPR)*, 2005, Vol. 2, pp. 60–65.

[71] K. Dabov, A. Foi, V. Katkovnik, and K. Egiazarian, "Image denoising by sparse 3-D transform-domain collaborative filtering," *IEEE Trans. Image Process.*, Vol. 16, No. 8, pp. 2080–2095, Aug. 2007.

[72] T. Teuberand A. Lang, "A new similarity measure for nonlocal filtering in the presence of multiplicative noise," *Comput. Stat. Data Anal.*, Vol. 56, No. 12, pp. 3821–3842, Dec. 2012.

[73] C. Kervrann, J. Boulanger, and P. Coupé, "Bayesian nonlocal means filter, image redundancy and adaptive dictionaries for noise removal," *in Proc. 1st Int. Conf. on Scale Space and Variational Methods in Computer Vision (SSVM)*, 2007, pp. 520–532.

[74] P. Coupe, P. Hellier, C. Kervrann, and C. Barillot, "Bayesian nonlocal means-based speckle filtering," in Proc. *5th IEEE Int. Symp. Biomedical Imaging: From Nano to Macro*, 2008, pp. 1291–1294.

[75] H. Zhong, Y. Li, and L. Jiao, "SAR image despeckling using Bayesian non-local means filter with sigma preselection," *IEEE Geosci. Remote Sensing Lett.*, Vol. 8, No. 4, pp. 809–813, July 2011.

[76] D. Gragnaniello, G. Poggi, and L. Verdoliva, "Classification based nonlocal SAR despeckling," *in Proc. Tyrrhenian Workshop on Advances in Radar and Remote Sensing*, 2012, pp. 121–125.

[77] L. I. Rudin, S. Osher, and E. Fatemi, "Nonlinear total variation based noise removal algorithms," Physica D, Vol. 60, No. 1–4, pp. 259–268, Nov. 1992.

[78] L. I. Rudin, P.- L . Lions, and S. Osher, *Multiplicative denoising and deblurring: Theory and algorithms*, in Geometric Level Set Methods in Imaging, Vision, and Graphics. New York: SpringerVerlag, 2003, pp. 103–119.

[79] G. Aubert and J. Aujol, "A variational approach to removing multiplicative noise," *SIAM J. Appl. Math.*, Vol. 68, No. 4, pp. 925–946, Dec. 2008.

[80] J. Shiand and S. Osher, "A nonlinear inverse scale space method for a convex multiplicative noise model," *SIAM J. Imaging Sci.*, Vol. 1, No. 3, pp. 294–321, Sept. 2009.

[81] Y.-M. Huang, M. K. Ng, and Y.-W. Wen, "A new total variation method for multiplicative noise removal," *SIAM J. Imaging Sci.*, Vol. 2, No. 1, pp. 20–40, Jan. 2009.

[82] S. Durand, J. Fadili, and M. Nikolova, "Multiplicative noise removal using L1 fidelity on frame coefficients," *J. Math. Imaging Vis.*, Vol. 36, No. 3, pp. 201–226, Mar. 2010.

[83] G. Steidland T. Teuber, "Removing multiplicative noise by Douglas-Rachford splitting methods," *J. Math. Imaging Vis.*, Vol. 36, No. 2, pp. 168–184, Feb. 2010.

[84] J. M. Bioucas-Diasand and M. A. T. Figueiredo, "Multiplicative noise removal using variable splitting and constrained optimization," *IEEE Trans. Image Process.*, Vol. 19, No. 7, pp. 1720–1730, July 2010.

[85] D. L. Donoho, "Compressed sensing," *IEEE Trans. Inform. Theory*, Vol. 52, No. 4, pp. 1289–1306, Apr. 2006.

[86] S. Foucher, "SAR image filtering via learned dictionaries and sparse representations," *in Proc. IEEE Int. Geoscience and Remote Sensing Symp. (IGARSS)*, 2008, Vol. I, pp. 229–232.

[87] M. Yangand and G. Zhang, "SAR image despeckling using overcomplete dictionary," *Electron. Lett.*, Vol. 48, No. 10, pp. 596–597, May 2012.

[88] Y. Hao, X. Feng, and J. Xu, "Multiplicative noise removal via sparse and redundant representations over learned dictionaries and total variation," *Signal Process.*, Vol. 92, No. 6, pp. 1536–1549, June 2012.

[89] Birgir Bjorn Saevarsson, Johannes R.Sveinsson and Jon Atli Benediktsson, "Combined Wavelet and Curvelet Denoising of SAR Images" *Proceedings of IEEE* 2004.

[90] Guozhong Chen and Xingzhao Liu, "Wavelet-Based Despeckling SAR Images Using Neighbouring Wavelet Coefficients." *Proceedings of IEEE* 2005.

[91] Wavelet Basics, Available: http://www.wavelet.org/tutorial/wbasic.htm

[92] S.Md.Mansoor Roomi, D.Kalaiyarasi, J.Goma Abhinaya and C.Bhavana, "Edge Preserving SAR image Despeckling", 2011 Third National Conference on Computer Vision, Pattern Recognition, Image Processing, and Graphics.

[93] Prabhishek Singh and Dr. Raj Shree, "Importance of DWT in Despeckling SAR Images and Experimentally Analyzing the Wavelet Based Thresholding Techniques", *published in International Journal of Engineering Sciences & Research Technology*, October, 2016, DOI: 10.5281/zenodo.160861.

[94] Abdullah Al Jumah, "Denoising of an Image Using Discrete Stationary Wavelet Transform and Various Thresholding Techniques", *Published Online February 2013, Journal of Signal and Information Processing*, 2013,4,33-41.

[95] Alka Vishwa and Shilpa Sharma, "Modified Method for Denoising the Ultrasound Images by Wavelet Thresholding", *Published Online June 2012 in MECS, I.J. Intelligent Systems and Applications*, 2012,Vol. 6,pp.25-30.

[96] Arun Dixit and Poonam Sharma, "A Comparative Study of Wavelet Thresholding for Image Denoising", *I.J. Image, Graphics and Signal Processing*, 2014, 12, pp.39-46 Published Online November 2014 in MECS, DOI: 10.5815/ijigsp.2014.12.06.

[97] Tinku Acharya and Ajoy K. Ray, "Image Processing Principles and Applications", 2005 edition A John Wiley & Sons, Mc., Publication.

[98] V.S.Frost *et al*, "A model for radar images and its application to adaptive digital filtering of multiplicative noise*", IEEE Trans. Pattern Anal. And Machine Intell*.,Vol. PAMI-4, pp.157-166. 1982.

[99] D. L. Donoho and I. M. Johnstone, "Adapting to unknown smoothness via wavelet shrinkage," *J. American Statistical Association*, Vol. 90, No. 432, pp. 1200–1224, Dec. 1995.

[100] D. L. Donoho and I. M. Johnstone, "Ideal spatial adaptation via wavelet shrinkage," Biometrika, Vol. 81, No. 3, pp. 425–455, Sep. 1994.

[101] Gregorio Andria, Filippo Attivissimo, Anna M. L. Lanzolla and Mario Savino, "A Suitable Threshold for Speckle Reduction in Ultrasound Images", *IEEE Transactions On Instrumentation And Measurement*, Vol. 62, No. 8, August 2013, Page(s): 2270 – 2279

[102] A. Achim, A. Bezerianos, and P. Tsakalides, "Novel bayesian multiscale method for speckle removal in medical ultrasound images," *IEEE Trans. Med. Imaging*, Vol. 20, No. 8, pp. 772–783, Aug. 2001.

[103] S. G. Chang, "Adaptive wavelet thresholding for image denoising and compression," *IEEE Trans. Image Processing*, Vol. 9, Sept. 2000, pp. 1532–1546.

[104] C. B. Burckhardt, "Speckle in ultrasound B-mode scans," *IEEE Trans. Sonics Ultrasonics*, Vol. 25, No. 1, pp. 1–6, Jan. 1978,

[105] Wavelet Noise Thresholding, Available: http://www.bearcave.com/misl/misl_tech/wavelets/noise.html

[106] MathWorks Documentation, wthresh(Soft or hard thresholding), Available: https://in.mathworks.com/help/wavelet/ref/wthresh.html

[107] MathsWorks Documentation, "Wavelet Family", Available: http://in.mathworks.com/help/wavelet/ug/wavelet-families-additional-discussion.html

[108] James S. Walker. "A Primer on Wavelets and Their Scientific Applications, Second Edition (Studies in Advanced Mathematics)" [English]. Published by Chapman And Hall, Crc (2008). Ch 2: Daubechies, Book (Online Source) Available: https://www.scribd.com/document/255294926/28851-a-Primer-on-Wavelets-and-Their-Scientific-Applications

[109] R. C. Gonzalez and R. E. Woods, "Digital Image Processing", second ed., Prentice-Hall, Inc., 2002.

[110] Nimrod Peleg, "The History and Families of Wavelets", Update: Dec. 2000, Available: cs.haifa.ac.il/~nimrod/Compression/Wavelets/w3families2000.pdf

[111] Prabhishek Singh and Dr. Raj Shree, "Statistical Modelling of Log Transformed Speckled Image", Published online in Vol. 14 No. 8 AUGUST 2016 *International Journal of Computer Science and Information Security*, (pp. 426-431).

[112] Esmaeilpour, M., and A. R. A. Mohammadi, " Analyzing the EEG Signals in Order to Estimate the Depth of Anesthesia using Wavelet and Fuzzy Neural Networks", Published in Vol. 4 No. 2 December 2016 in *International Journal of Interactive Multimedia and Artificial Inteligence*, (pp. 12-15).

[113] Carlos Javier Broncano Mateos , Carlos Pinilla Ruiz , Ruben Gonzalez Crespo and Andrew Gaspar Castillo Sanz, "Relative Radiometric Normalization of Multitemporal images", Published online in *International Journal of Interactive Multimedia and Artificial Inteligence*, ISSN-e 1989-1660, Vol.1, No. 3, pp. 54-59, 2010.